ACS APPLIED MATERIALS & INTERFACES

Research Article

www.acsami.org

Synergetic Influences of Mixed-Host Emitting Layer Structures and Hole Injection Layers on Efficiency and Lifetime of Simplified Phosphorescent Organic Light-Emitting Diodes

Tae-Hee Han,[†] Young-Hoon Kim,[†] Myung Hwan Kim,[‡] Wonjun Song,[‡] and Tae-Woo Lee*[,†]

[†]Department of Materials Science and Engineering, Pohang University of Science and Technology (POSTECH), 77 Cheongam-ro, Nam-gu, Pohang, Gyungbuk 790-784, Republic of Korea

[‡]Samsung Display Co., Ltd., 95 Samsung 2-ro, Giheung-gu, Yongin-city, Gyeonggi-Do 446-711, Republic of Korea

Supporting Information

ABSTRACT: We used various nondestructive analyses to investigate various host material systems in the emitting layer (EML) of simple-structured, green phosphorescent organic light-emitting diodes (OLEDs) to clarify how the host systems affect its luminous efficiency (LE) and operational stability. An OLED that has a unipolar single-host EML with conventional poly(3,4-ethylenedioxythiophene):poly(styrenesulfonate) (PEDOT:PSS) showed high operating voltage, low LE (~26.6 cd/A, 13.7 lm/W), and short lifetime (~4.4 h @ 1000 cd/m^2). However, the combined use of a gradient mixed-host EML and a molecularly controlled HIL that has increased surface work function (WF) remarkably decreased operating voltage and improved LE (~68.7 cd/A, 77.0 lm/W) and lifetime (~70.7 h @ 1000 cd/m^2). Accumulated charges at the injecting interfaces and formation of a narrow recombination zone close to the interfaces are the major factors that accelerate degradation of charge injection/transport and electroluminescent properties of OLEDs, so achievement of simple-structured OLEDs with high efficiency and long lifetime requires facilitating charge injection and balanced transport into the EML and distributing charge carriers and excitons in EML.

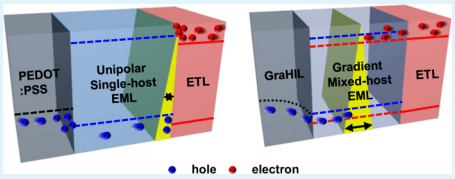

KEYWORDS: *organic light-emitting diodes, simple structure, mixed host, degradation mechanism, lifetime, nondestructive analysis, transient electroluminescence, capacitance−voltage*

INTRODUCTION

Organic light-emitting diodes (OLEDs) have promising applications in large-area, full-color, flat-panel displays and solid-state lighting sources.[1−7] However, the electrical and luminescent properties of simplified OLEDs are degraded rapidly at high luminance; these problems must be solved before OLEDs can be adopted for practical use. Extrinsic factors that affect OLED degradation have been identified and controlled by protecting devices from the ambient environment, but intrinsic mechanisms of long-term degradation remain unclear.[8−12] Because intrinsic OLED degradation mechanisms can depend on device structures and materials used, any understanding of degradation mechanisms can be restricted to particular device structures and material systems.[12] Development of multilayered device structures has led to significant improvements in electroluminescent efficiency and operational stability of small-molecule OLEDs.[13−16] Insertion of many functional layers in multilayered OLEDs can facilitate charge carrier injection, transport, and blocking to achieve balanced carrier injection, transport, and effective confinement in the emitting layer (EML), thereby improving both device efficiency and lifetime.[13−16] However, the standard multilayered structure of OLEDs inevitably entails high fabrication cost because the standard method to deposit a small-molecule layer is vacuum thermal evaporation. To meet the objective of low-cost mass-production of OLEDs, simplified small-molecule OLEDs with high efficiency and stability comparable to those of conventional multilayered OLEDs must be developed. However, simple-structured OLEDs without a carrier transporting layer suffer from insufficient carrier injection and poor transport to the EML.[16] Furthermore, because host materials that have high triplet energy level for phosphorescent dopants generally have a large energy band gap, simplification of phosphorescent OLED structure can cause severe charge injection difficulty, thereby increasing their operating voltage and decreasing their luminous efficiency (LE). Charge imbalance in the EML additionally increases nonradiative recombination including triplet−triplet annihilation (TTA) and triplet-polaron annihilation (TPA), and thus, simple-structured phosphorescent OLEDs that can form a narrow recombination zone in EML can have large efficiency roll-off and operational instability.[17−19]

In this study, we quantified how host material systems in the EML affect the electroluminescent properties and their operational degradations in phosphorescent OLEDs that have a simplified structure of [anode/hole injection layer (HIL)/EML/electron transporting layer (ETL)/cathode]. Two kinds of variables were used for this study: hole injection layers with

Received: December 3, 2015
Accepted: February 16, 2016
Published: February 16, 2016

DOI: 10.1021/acsami.5b11791
ACS Appl. Mater. Interfaces 2016, 8, 6152−6163

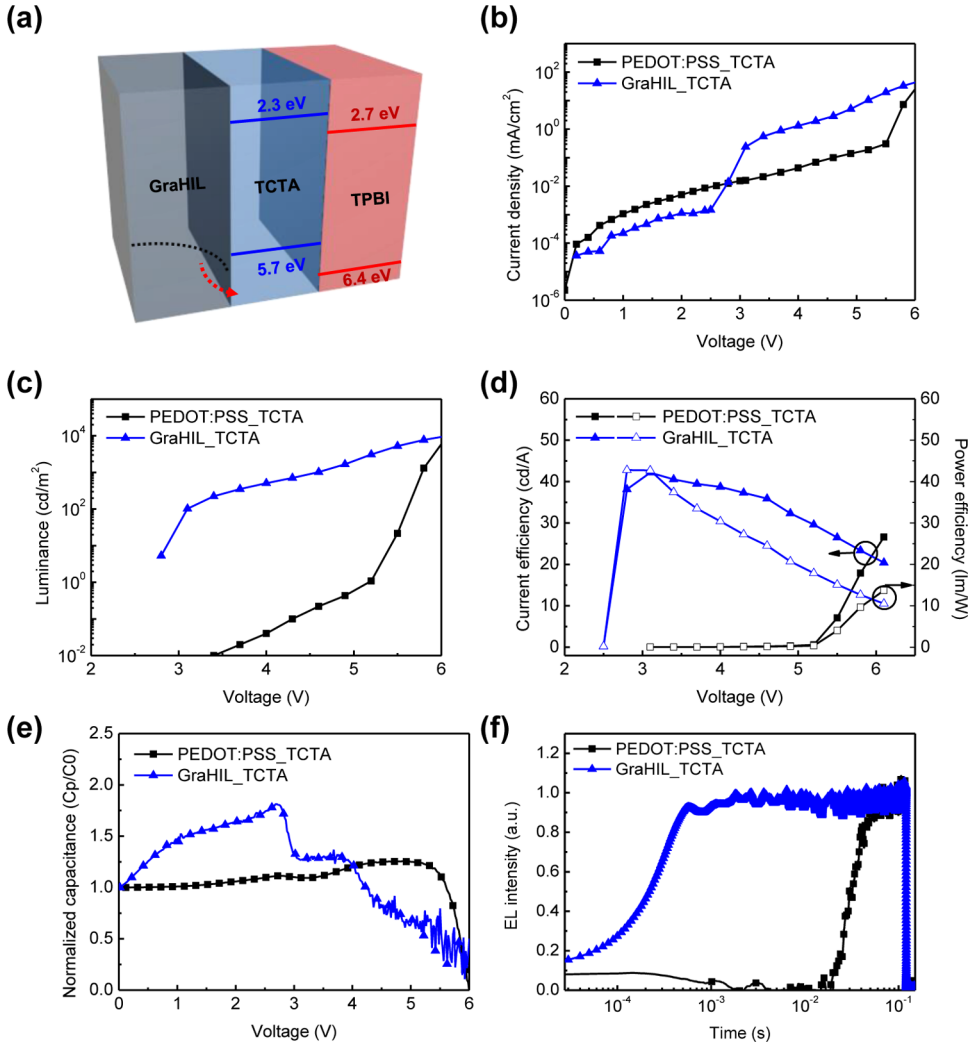

Figure 1. (a) Schematic energy band diagram of HIL, EML, and ETL in simple-structured green phosphorescent OLEDs using a TCTA single-host EML, (b) current densities, (c) luminance, (d) current (closed symbols) and power (open symbols) efficiencies, (e) normalized capacitances ($C_p C_0^{-1}$) versus voltage, and (f) transient EL rising characteristics of simple-structured phosphorescent OLEDs that use a TCTA single-host EML with GraHIL or PEDOT:PSS as HIL.

different work function (WF) and host systems of EML using various host materials. Because the simple device structure does not have a hole transporting layer (HTL), a large energy barrier for hole injection forms at the interface between HIL and EML. To investigate the effect of this hole injection energy barrier, we used two kinds of polymeric HILs with different WF. The surface WF of the HIL can be tuned by using polymer composition HIL (GraHIL) of poly(3,4-ethylenedioxythiophene):poly(styrene sulfonate) (PEDOT:PSS) and tetrafluoro-ethylene-perfluoro-3,6-dioxa-4-methyl-7-octene-sulfonic acid copolymer, a perfluorinated ionomer (PFI). Because PFI that has higher ionization potential than that of PEDOT:PSS is preferentially positioned near the surface of the film by self-organization, the final WF gradually increases from the anode to the surface, and the surface WF increases (PEDOT:PSS ~5.0−5.2 eV, GraHIL ~5.95 eV).[6,12,16,20] To study influences of EML in simple-structured phosphorescent OLEDs, by using various host materials that have different charge carrier transport characteristics and energy levels, we also provided four host systems for the EML: (1) unipolar single-host, (2) bipolar single-host, (3) mixed-host, and (4) gradient mixed-host (GMH). The fabricated devices were characterized by using various kinds of nondestructive analyzing methods including current−voltage−luminance ($I-V-L$), capacitance−voltage ($C-V$), transient electroluminescence (EL), and operational lifetime to systematically identify causes of OLED properties and their degradation characteristics.

EXPERIMENTAL SECTION

OLED Fabrication. Indium tin oxide (ITO; WF ~4.8 eV) on glass substrate (2 × 3 mm active area) was used and cleaned in ultrasonic baths using acetone and isopropyl alcohol, each for about 15 min before use. The ITO/glass substrate was treated with ultraviolet ozone for 15 min; then, polymeric HILs including PEDOT:PSS and GraHIL were spin-coated. The GraHIL was composed of PEDOT:PSS (CleviosTM P VP AI4083) and a tetrafluoroethylene-perfluoro-3,6-dioxa-4-methyl-7-octene-sulfonic acid copolymer (CAS number: 31175-20-9) (Sigma-Aldrich Inc.) in 1:3.6 weight ratio (Surface WF of HIL: ~5.95 eV).[6,20] Then, 50 nm-thick polymeric HIL films were deposited and immediately annealed on a hot plate at 150 °C for about 30 min under ambient condition. To form single-host EMLs, tris(4-carbazoyl-9-ylphenyl)amine (TCTA) and 4,4′-bis(9-carbazolyl)-biphenyl (CBP) were deposited, respectively. To form mixed-host EMLs, TCTA:CBP and TCTA:1,3,5-tris(*N*-phenylbenzimidizol-2-yl)benzene (TPBI) were codeposited at 1:1 weight ratio. To form

DOI: 10.1021/acsami.5b11791
ACS Appl. Mater. Interfaces 2016, 8, 6152−6163

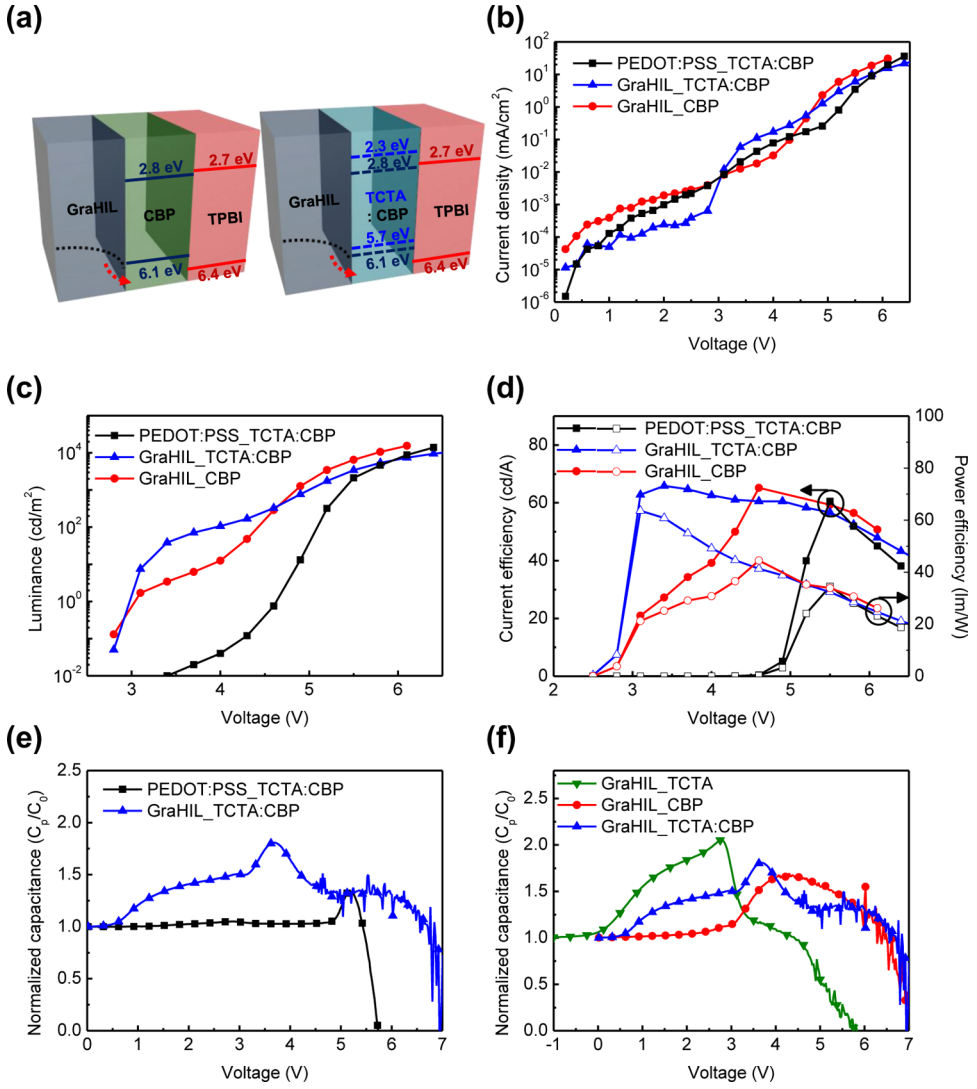

Figure 2. (a) Schematic energy band diagrams of HIL, EML, and ETL in simple-structured green phosphorescent OLEDs using a CBP single-host and a TCTA:CBP mixed-host EML, (b) current densities, (c) luminance, (d) current (closed symbols) and power (open symbols) efficiencies, and normalized capacitances (C_p C_0^{-1}) versus voltage characteristics of simple-structured phosphorescent OLEDs that use (e) a TCTA:CBP mixed-host EML with GraHIL or PEDOT:PSS as a HIL and (f) TCTA, CBP single-host, and TCTA:CBP mixed-host EMLs with GraHIL.

the GMH-EML, we gradually controlled codeposition rates of TCTA and TPBI, respectively, with five individual deposition steps, which were programmed in our automatic thermal evaporator (Figure S1). The deposition rate of TCTA (TPBI) was changed from 0.9 Å/s to 0.1 Å/s (from 0.1 to 0.9 Å/s) with 0.2 Å/s step while maintaining the total deposition rate of TCTA and TPBI at 1 Å/s. In all devices, a 55 nm-thick TPBI layer was used as an ETL and 8 wt % of bis(2-phenylpyridine)iridium(III)-acetylacetonate ($Ir(ppy)_2(acac)$) was added to the host material as a green-emitting phosphorescent dopant; then, 1 nm-thick LiF and 130 nm-thick Al were deposited sequentially as an electron injection layer and a cathode, respectively. All layers of the OLEDs were deposited using a vacuum thermal evaporator under high vacuum (<5 × 10^{-7} Torr) according to their respective device structures. All fabricated OLEDs were protected by glass encapsulation using a UV resin with a getter.

OLED Characterizations. *I*–*V*–*L* characteristics and EL spectra were measured using a source-measurement unit (Keithley 236) and a spectro-radiometer (Minolta CS2000). *C*–*V* characteristics were measured using an electrochemical impedance spectroscope (Biologic SP-300). All the devices were biased from 0 to 8 V at constant frequency (1000 Hz) in darkness. Transient EL characteristics were measured by using a pulse generator (HP 8116A) to apply a constant square electrical pulse (100 ms width; 10 Hz frequency) to devices. Emitted light was detected using a photon-counting-spectro-fluorometer (ISS PC1), and the EL rising output signal was monitored using an oscilloscope (Agilent infiniium S4832B DSO).

RESULTS AND DISCUSSION

Single-Host Emitting Layer. We fabricated simple-structured OLEDs that use a TCTA single-host EML with PEDOT:PSS or GraHIL as a HIL. Because TCTA has a deep highest occupied molecular orbital (HOMO) energy level (~5.7 eV),[21] a large hole injection energy barrier forms between a PEDOT:PSS HIL and TCTA in the EML, so an OLED with PEDOT:PSS cannot easily inject holes into the EML. In contrast, in an OLED with a GraHIL, the improved surface WF of the GraHIL (~5.95 eV) yields a good energy level alignment between the HIL and the EML, so hole injection is facilitated (Figure 1a).[6,12,16,20] Therefore, devices with the GraHIL showed a rapid increase of current density, luminance at low voltages (low turn-on voltage (V_{to}: ~2.5 V) defined as the voltage required to emit ~1 cd m^{-2}), whereas the device with PEDOT:PSS showed much lower current density, luminance characteristics much higher (V_{to} ~5.5 V) than those

DOI: 10.1021/acsami.5b11791
ACS Appl. Mater. Interfaces 2016, 8, 6152–6163

of the device with GraHIL (Figure 1b,c). This result indicates that overcoming the large energy barrier between PEDOT:PSS and TCTA requires much higher applied forward bias compared with GraHIL. In simple-structured OLEDs that use TCTA single-host, use of the GraHIL increased hole injection significantly and therefore increased current efficiency (CE) to ∼42.2 cd/A and power efficiency (PE) to ∼42.8 lm/W compared to those with PEDOT:PSS (CE ∼ 26.6 cd/A, PE ∼ 13.7 lm/W; Figure 1d).

The $C-V$ characterization directly represents the charge carrier dynamics of OLEDs at varying applied bias. Rapid ascent of capacitance (C_p) from geometric capacitance (C_0) in the dark regime implies injection and accumulation of major charge carriers, and descent of C_p after a peak means a decrease of accumulated charges due to balanced recombination of accumulated major carriers and injected minor carriers in the OLEDs.[12,22] Therefore, the voltage at the peak capacitance (V_{peak}) can be matched with the voltage required to let major and minor carriers meet in the EML, and thus, the V_{peak} in $C-V$ characterizations is generally similar to the V_{to} in $I-V-L$ characterization. We measured the normalized capacitance (C_p C_0^{-1}) during sweeps at a range of voltages. In the device with GraHIL, C_p C_0^{-1} increased rapidly with voltage when voltage was low and decreased at voltages > V_{peak} ∼2.5 V; by comparison, in the device with PEDOT:PSS, C_p C_0^{-1} increased more slowly, reached a lower maximum, and decreased after higher V_{peak} (Figure 1e). The V_{peak} of the device with PEDOT:PSS (∼5.5 V) was much higher than that with GraHIL and also similar to V_{to} in $I-V-L$ characterizations. Because TCTA which solely forms the EML is a unipolar hole transporting host material with high hole mobility ($\sim 3 \times 10^{-4}$ cm^2 V^{-1} s^{-1}),[23] holes can be regarded as the major carriers in these simple-structured OLEDs. Holes can be easily injected into the EML through the GraHIL; they accumulate at the EML/ETL interface at low applied bias and, then, recombine with electrons injected from the cathode. In contrast, the device with PEDOT:PSS requires much higher bias to accumulate holes for recombination due to its insufficient hole injection capability.

During transient EL characterization, EL rising also shows charge carrier injection and transport characteristics: the delay time (t_d) (i.e., time between onset of the square voltage pulse and onset of EL rise) can be considered as the time required until leading fronts of major and minor charge carriers meet, and the saturation time (t_s) (defined in this experiment as time required to reach ∼90% of saturated EL intensity) can be thought as the time required to build up sufficient minority charge carriers to form dynamic equilibrium in the OLEDs.[24,25] In transient EL characterizations, the OLED with GraHIL showed much earlier EL rising and saturation ($t_d \sim 7 \times 10^{-5}$ s; $t_s \sim 5.5 \times 10^{-4}$ s) than did those with PEDOT:PSS ($t_d \sim 1.5 \times 10^{-2}$ s; $t_s \sim 6 \times 10^{-2}$ s) (Figure 1f). A transient EL result in the simple-structured OLED that uses a TCTA single-host EML also means that the device with GraHIL much more effectively injects and transports holes to the recombination zone and more efficiently recombines them with electrons transported from a cathode than does a device with PEDOT:PSS. The $I-V-L$, $C-V$, and transient EL results all concur that, because a simple-structured OLED using a TCTA single-host EML forms a large hole injection energy barrier without a HTL, this energy barrier has a critical influence on the electroluminescent properties of devices.

We also fabricated simple-structured OLEDs using 4,4′-bis(9-carbazolyl)-biphenyl (CBP) as a bipolar host material which has high hole ($\sim 2 \times 10^{-3}$ cm^2 V^{-1} s^{-1}) and electron ($\sim 3 \times 10^{-4}$ cm^2 V^{-1} s^{-1}) mobility (Figure 2a).[23] Although CBP has bipolar transporting characteristics, its HOMO energy level is deeper (∼6.1 eV) than that of TCTA,[26] and thus, a larger energy barrier for hole injection forms at the interface between HIL and EML than does TCTA in the simple-structured OLEDs (Figure 2a). Because the energy barrier that should be overcome during carrier injection was increased, the V_{to} increased in OLEDs that use a CBP single-host EML with GraHIL (∼3.1 V) compared with those that use TCTA (Figure 2b,c). Furthermore, in OLEDs that use CBP, hole injection is difficult due to a large hole injection energy barrier under low voltages, so these devices have limited current density and luminance at low voltage regime. However, CE and PE of the OLED that uses a CBP single-host EML with GraHIL were improved (∼65.2 cd/A and 44.5 lm/W) at high voltage regime compared with those that use TCTA (Figure 2d). This improvement in device efficiencies by using CBP can be attributed to bipolar transporting capability of CBP; this capability improves the balance of charge transport in the EML after overcoming a hole injection energy barrier formed by CBP at high voltages. Furthermore, because bipolar characteristics of EML can more easily distribute charge carriers and excitons in EML, a broader recombination zone can be formed in CBP single-host compared to TCTA, thereby reducing the non-radiative recombination.

Mixed-Host Emitting Layer. When the hole transporting TCTA and the bipolar transporting CBP are codeposited (1:1 weight ratio) to form a TCTA:CBP mixed-host EML, the shallower HOMO energy level of the TCTA (∼5.7 eV) than that of CBP (∼6.1 eV) can contribute to improving the energetic favorability of hole injection from HIL to the TCTA in EML at low voltages compared with that obtained using a CBP single-host EML. The higher current density and luminance of OLED that uses the TCTA:CBP mixed-host EML with GraHIL at low voltages compared with those using single CBP emphasizes the advantage of reducing energy barrier by adding the TCTA to the EML (Figure 2b,c). The device that uses the CBP single-host had higher current density and luminance after overcoming a large energy barrier at high voltages than did those that used TCTA:CBP; this difference can be understood by considering that CBP has higher hole and electron mobility than those with TCTA. As a result, the OLED that uses TCTA:CBP mixed-host EML with GraHIL exhibited improved CE ∼ 65.9 cd/A and PE ∼ 63.6 lm/W at the same time, whereas the OLED that uses a CBP single-host had lower PE (∼44.5 lm/W) due to inefficient hole injection to CBP at low voltages (Figure 2d). A significant increase of PE also can be attributed to reduction of the energy barrier effect of the TCTA addition at low voltages. In contrast, using the TCTA:CBP with PEDOT:PSS did not significantly improve current density and luminance characteristics (Figure 2b,c) because PEDOT:PSS still can not efficiently inject holes even into the TCTA (Figure 1).

In $C-V$ characterization, C_p C_0^{-1} increased sharply at low voltages (V_{peak}: ∼3.5 V) in the device with GraHIL but increased slowly at high voltages (V_{peak}: ∼5 V) in the device with PEDOT:PSS (Figure 2e); this result clearly shows that devices with GraHIL and PEDOT:PSS differ greatly in majority carrier (i.e., holes in these devices) injection characteristics. The differences in the $C-V$ characteristics of the devices that use

DOI: 10.1021/acsami.5b11791
ACS Appl. Mater. Interfaces 2016, 8, 6152−6163

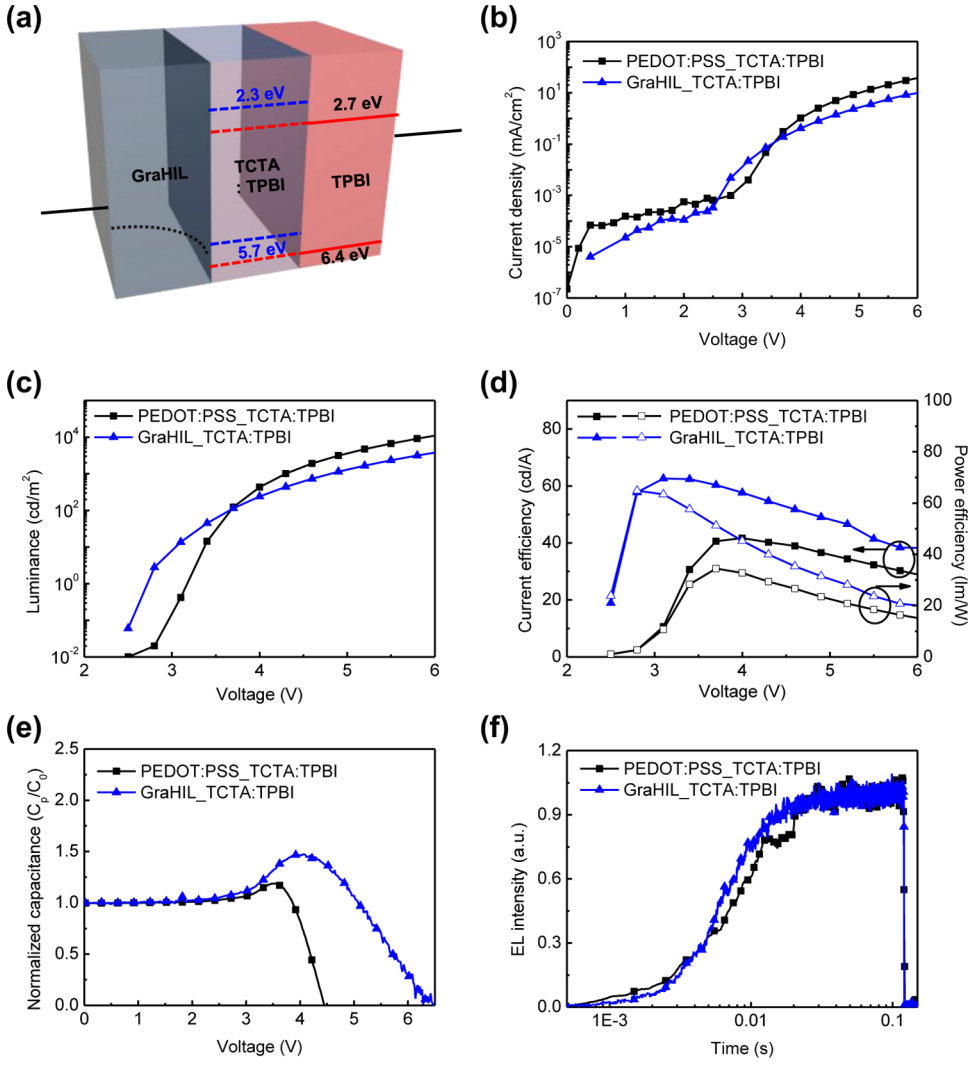

Figure 3. (a) Schematic energy band diagram of HIL, EML, and ETL in simple-structured green phosphorescent OLEDs using a TCTA:TPBI mixed-host EML, (b) current densities, (c) luminance, (d) current (closed symbols) and power (open symbols) efficiencies, (e) normalized capacitances (C_p C_0^{-1}) versus voltage, and (f) transient EL rising characteristics of simple-structured phosphorescent OLEDs that use the TCTA:TPBI mixed-host EML with GraHIL or PEDOT:PSS as a HIL.

TCTA, CBP, and TCTA:CBP EML with the GraHIL suggest obviously that charge carrier injection, transport, and blocking characteristics strongly depend on the materials used in the EML (Figure 2f). OLEDs that use the TCTA single-host EML with GraHIL showed the earliest and highest increase of C_p C_0^{-1} (V_{peak}: ~2.8 V) at low voltages and rapid decrease of C_p C_0^{-1} as voltage increased, whereas OLEDs that use the CBP single-host EML had the latest increase of C_p C_0^{-1} (V_{peak}: ~4.2 V), and C_p C_0^{-1} did not rapidly decrease even at high voltages. The relatively late decrease of C_p C_0^{-1} implies that GraHIL has excellent electron blocking characteristics because more electrons can be transported and reach the HIL due to the presence of CBP which has high electron mobility in the EML; the surface enriched insulating PFI layer on GraHIL can effectively block electrons that are transported through the EML and thereby effectively confine the charge carriers in the EML and consequently increase LEs of the device with GraHIL.[16,20] Therefore, the decrease in C_p C_0^{-1} was slower in OLEDs that use the CBP single-host EML with GraHIL than in OLEDs that use PEDOT:PSS (Figure S2). Consequently, in $C-V$ measurement, the OLED that uses the TCTA:CBP showed averaged $C-V$ characteristics of those that use TCTA and CBP single-host EML; holes can be injected at low voltages (V_{peak}: ~3.6 V) due to TCTA, and C_p C_0^{-1} decreases slowly at high voltages due to CBP in the EML, thereby improving both CE and PE.

Although the CBP has bipolar transporting property, the device with TCTA:CBP mixed-host EML can be also considered as a dominantly hole-transporting device because both TCTA and CBP have higher hole mobilities than their electron mobilities. The devices that use the TCTA single-host EML or the TCTA:CBP mixed-host EML showed undesirable $I-V-L$ characteristics with PEDOT:PSS because majority carriers (i.e., holes) can not be easily injected into the EML due to large hole injection barriers (Figures 1b,d, and 2b,d). $C-V$ and transient EL characterizations also supported very inefficient hole injection of devices with PEDOT:PSS. On the other hand, the GraHIL greatly improved hole injection capability and $I-V-L$ characteristics of simple-structured OLEDs (Figures 1 and 2). Therefore, the combined use of the PEDOT:PSS HIL and the hole dominant EMLs with much

DOI: 10.1021/acsami.5b11791
ACS Appl. Mater. Interfaces 2016, 8, 6152−6163

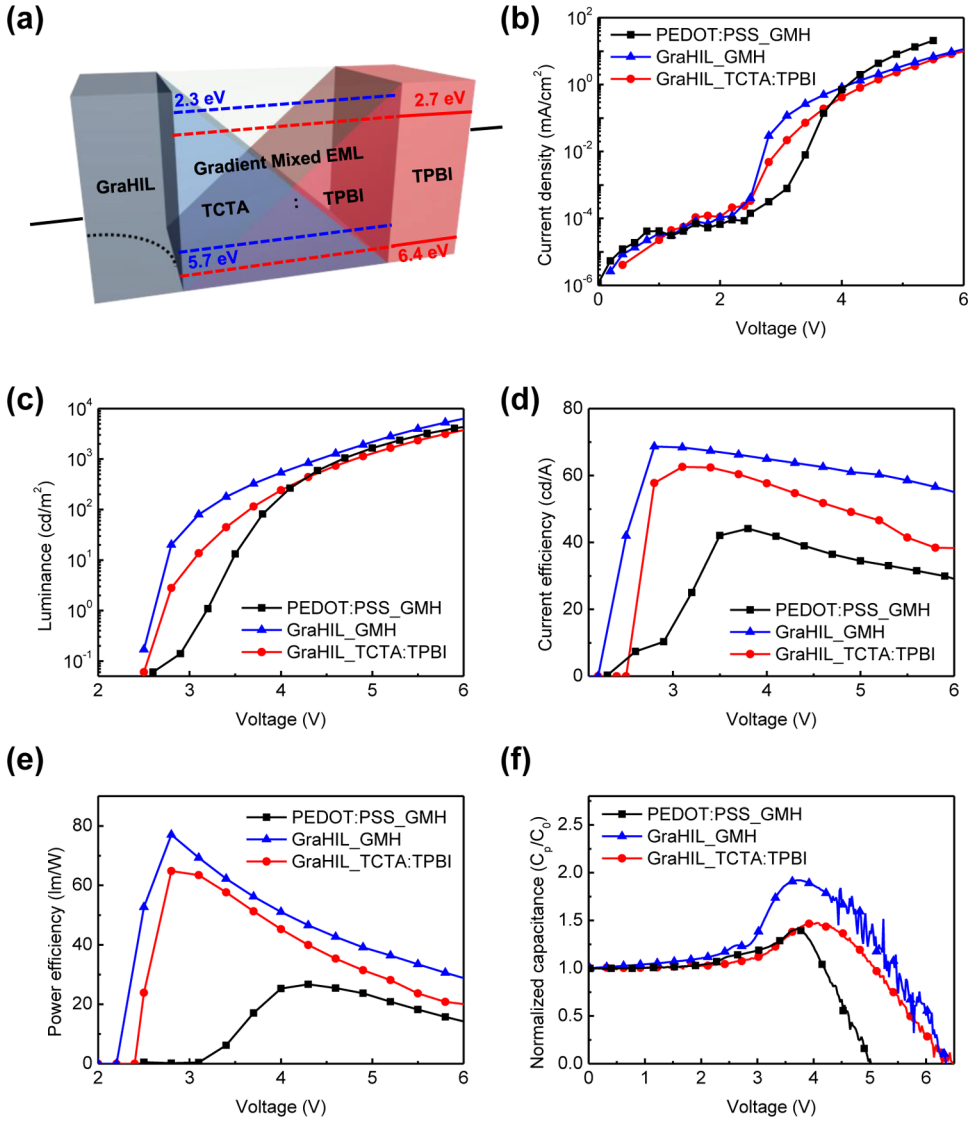

Figure 4. (a) Schematic energy band diagrams of HIL, EML, and ETL in simple-structured green phosphorescent OLEDs using a TCTA:TPBI gradient mixed-host EML, (b) current densities, (c) luminance, (d) current, (e) power efficiencies, and (f) normalized capacitances (C_p C_0^{-1}) versus voltage characteristics of simple-structured phosphorescent OLEDs that use a TCTA:TPBI gradient mixed-host EML with GraHIL or PEDOT:PSS as a HIL.

deeper HOMO energy level than WF of PEDOT:PSS does not act suitably in the simple-structured phosphorescent OLEDs.

We mixed two different unipolar host materials, hole-transporting TCTA and electron-transporting TPBI, to investigate influences of bipolar mixed-host EML on simple-structured OLEDs (Figure 3a). Electrons can be easily injected through electron-transporting TPBI in TCTA:TPBI mixed-host EML. As a result, simple-structured OLEDs that use TCTA:TPBI with PEDOT:PSS showed significant improvement in current density and luminance characteristics (Figure 3b,c); although PEDOT:PSS can not effectively overcome the hole injection energy barrier between PEDOT:PSS and TCTA, an increase in electron injection and transport from the ETL substantially increases current density and luminance in an OLED with PEDOT:PSS. Much higher current and luminance characteristics of the device with PEDOT:PSS at high voltages than those with GraHIL means that electrons dominantly influence overall current and luminance characteristics in OLEDs that use the TCTA:TPBI mixed-host EML, because GraHIL effectively blocks the electrons transported from the EML. The GraHIL can easily inject holes through the TCTA into the EML at low voltages, and the bipolar transporting property of TCTA:TPBI EML can provide balanced charge transport and formation of a broad recombination zone; therefore, devices with GraHIL had relatively high CE ~ 62.6 cd/A and PE ~ 57.8 lm/W compared with those of devices with PEDOT:PSS (CE ~ 41.7 cd/A; PE ~ 34.5 lm/W) (Figure 3d). Due to the unipolar hole transporting characteristics of the TCTA single-host EML, OLEDs that use TCTA host can form a narrow recombination zone very close to the EML/ETL interface whereas bipolar transport in TCTA:TPBI can broaden and shift the recombination zone away from the EML/ETL interface; this different formation of recombination zones in the two EMLs can reduce nonradiative exciton quenching including TTA and TPA.[17−19] Although CE and PE of the devices with the PEDOT:PSS were lower than those with the GraHIL, the contribution of significantly increased electron injection in the TCTA:TPBI mixed-host EML also greatly reduced operating

DOI: 10.1021/acsami.5b11791
ACS Appl. Mater. Interfaces 2016, 8, 6152−6163

voltage (V_{to}: ~3.2 V) and improved CE and PE (~41.7 cd/A and 34.5 lm/W) at the same time. $C-V$ and transient EL characterization also showed improved charge carrier balance in an OLED that uses the TCTA:TPBI EML with PEDOT:PSS unlike those using other host systems. Although the increase of $C_p\ C_0^{-1}$ in the device with PEDOT:PSS was slightly slower and lower than that with GraHIL, $C_p\ C_0^{-1}$ was decreased earlier after V_{peak} (~3.5 V) than that with GraHIL (V_{peak}: ~4 V) unlike those with other EMLs that use other host systems (Figure 3e). These differences in $C_p\ C_0^{-1}$ and V_{peak} also can be explained by the greatly enhanced electron injection through the TCTA:TPBI mixed-host EML and excellent electron blocking capability of GraHIL. The EL rising of the device with PEDOT:PSS also showed similar t_d and t_s to those with GraHIL in transient EL measurements (Figure 3f). These results demonstrate that use of the bipolar TCTA:TPBI mixed-host EML significantly compensated for inefficient hole injection of PEDOT:PSS by greatly enhancing the electron injection and transport into the EML.

Gradient Mixed-Host Emitting Layer. To further facilitate charge carrier injection and transport into the bipolar mixed-host EML, we used a GMH-EML formed by gradually decreasing the ratio of TCTA to TPBI from the HIL/EML to the EML/ETL interface (Figures 4a and S1). Because, in GMH-EML, only a little TPBI is deposited at the hole-injecting interface and only a little TCTA is deposited at the electron-injecting interface, the ease with which charge carriers can be injected into EML is increased with very small hindrance by the deep HOMO energy level of TPBI (6.4 eV) for holes and low lowest unoccupied molecular orbital (LUMO) energy level of TCTA (2.3 eV) for electrons.[21,27] Due to enhanced charge carrier injection at both interfaces of the GMH-EML, simple-structured OLEDs that use the GMH-EML with GraHIL showed higher current density and luminance characteristics (V_{to}: ~2.6 V) especially at low voltages than did the device that uses the TCTA:TPBI mixed-host EML (V_{to}: ~2.7 V) (Figure 4b,c). Furthermore, using the GMH-EML can broaden and shift the recombination zone toward the center of the EML and, thus, can effectively reduce the nonradiative recombination of excitons at the EML/ETL interfaces and, as a consequence, increase LEs and reduce the efficiency roll-off at high luminance. The change of EL spectra of simple-structured OLEDs that use various kinds of host systems in EML can support the shifts of the recombination zone in EML as we estimated in this work. The EL spectra gradationally red-shifted in the order of TCTA unipolar single-host < CBP bipolar single-host < TCTA:TPBI mixed-host < TCTA:TPBI GMH, which implies that the recombination zone gradually shifted from the EML/ETL interface to the center of the EML (Figure S3).[28] As a result, although current densities of devices that use GMH and mixed-host EML were similar at high voltages, the luminance of the device that uses the GMH-EML was higher even at high voltages, so the CE and PE of the device using the GMH-EML were higher (~68.7 cd/A and 77.0 lm/W) than those using general mixed-host EML (~62.6 cd/A and 57.8 lm/W; Figure 4d,e and Table 1). The large contrast between the PEs of devices that use GMH and mixed-host EML can also be attributed to combination of the enhanced charge injection at low voltage and broad recombination zone at the center of EML by using the GMH. The increase of $C_p\ C_0^{-1}$ at low voltage was larger and V_{peak} (~3.6 V) was smaller in the device that uses the GMH-EML than in the device that uses the mixed-host EML (V_{peak}: ~3.9 V) respectively, (Figure 4f); these differences prove that both hole and electron injection into the GMH-EML are more effective than into the mixed-host EML.

Table 1. Device performances of simple-structured OLEDs that use various kinds of EMLs

structure	V_{to} (V)	CE_{max} (cd/A)	PE_{max} (lm/W)	L_{50} (h)
		TCTA		
PEDOT:PSS	5.5	26.6	13.7	4.4
GraHIL	2.5	42.2	42.8	
		CBP		
PEDOT:PSS	4.1	55.1	26.9	
GraHIL	3.1	65.2	44.5	
		TCTA:CBP		
PEDOT:PSS	4.6	60.5	34.5	
GraHIL	2.9	65.9	63.6	
		TCTA:TPBI		
PEDOT:PSS	3.2	41.7	34.5	
GraHIL	2.7	62.6	57.8	
		TCTA:TPBI GMH		
PEDOT:PSS	3.1	44.1	26.7	47.8
GraHIL	2.6	68.7	77.0	70.7

Nondestructive Analyses on OLED Degradation. Investigation of electrical and EL properties in OLEDs proved that the TCTA:TPBI GMH-EML system improves both charge carrier injection and transport and forms a broad recombination zone at the center of EML in simple-structured phosphorescent OLEDs. The GraHIL also significantly enhances hole injection by reducing energy barrier between the HIL and the EML compared with the PEDOT:PSS HIL. To verify degradation characteristics of simple-structured OLEDs according to influences of GMH-EML and GraHIL, we used nondestructive analysis methods ($C-V$, transient EL, $I-V-L$, and lifetime measurement) to analyze three selected OLEDs: (i) the OLED with the TCTA single-host EML and the PEDOT:PSS HIL as a control device, (ii) the OLED with the TCTA:TPBI GMH-EML and the PEDOT:PSS HIL to see influences of the GMH system compared with the control device, and (iii) the OLED with GMH-EML and GraHIL to see influences of the combined use of GMH-EML and GraHIL compared to the others. The measurements were conducted at three different degradation stages: fresh, 25%, and 50% degraded from initial luminance under constant current operation.

In $C-V$ characterization, OLEDs that use the TCTA single-host EML with PEDOT:PSS showed the largest change under device degradation (Figure 5a). In these devices, the ascent of $C_p\ C_0^{-1}$ gradually decreased at low voltage (<3 V) under device degradation; this means that operation of the device degrades injection of major charge carriers (i.e., holes) from anode to EML. Furthermore, the V_{peak} also showed a gradual and significant increase (4 to 6.82 V); this result indicates that both charge carrier injection and transport in this device were severely degraded under device operation because capacitance can be decreased only after charge carriers recombine maintaining charge balance in the EML. In the OLED that uses GMH-EML with PEDOT:PSS, the peak capacitance decreased; V_{peak} increased slightly under device degradation, but the changes in $C-V$ characteristics were much smaller than those in the OLED that uses the TCTA single-host EML. However, the decrease of $C_p\ C_0^{-1}$ after peak capacitance became retarded gradually (Figure 5b); the crossover voltage (V_c) defined as the voltage required to make $C_p\ C_0^{-1} = 0$ after

DOI: 10.1021/acsami.5b11791
ACS Appl. Mater. Interfaces 2016, 8, 6152−6163

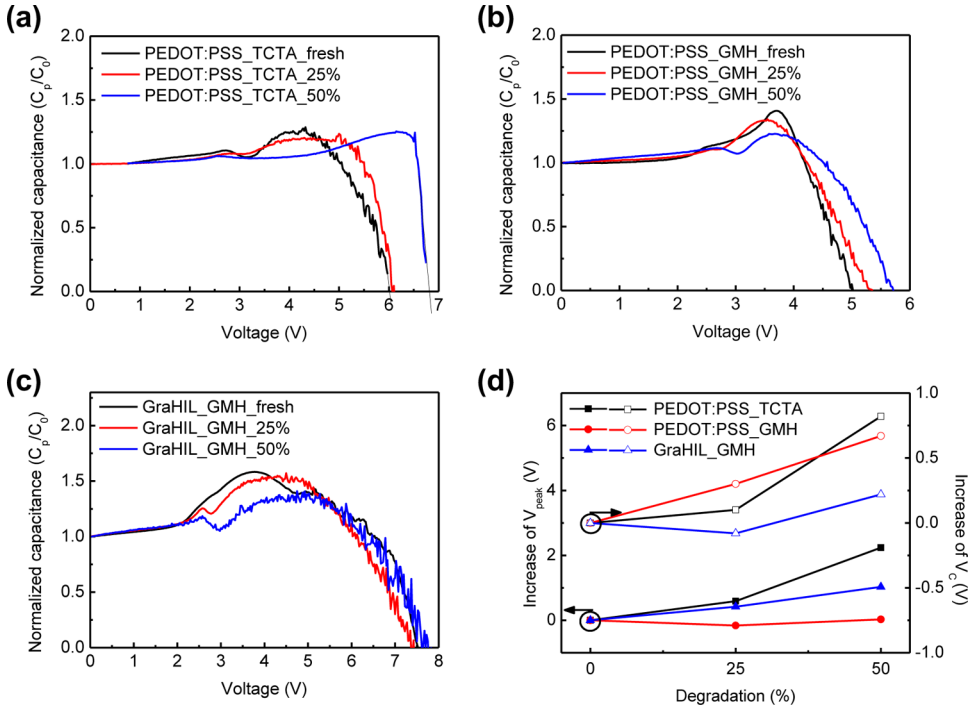

Figure 5. Normalized capacitance ($C_p\ C_0^{-1}$) versus voltage characteristics of OLEDs that use (a) the TCTA single-host with PEDOT:PSS and TCTA:TPBI gradient mixed-host EML with (b) PEDOT:PSS, (c) GraHIL at various degraded stages (fresh, 25%, and 50% degraded stages of initial luminance under constant current operation), and (d) changes of voltage at a peak capacitance (V_{peak}) (closed symbols) and crossover voltage (V_c) (open symbols) versus device degradation.

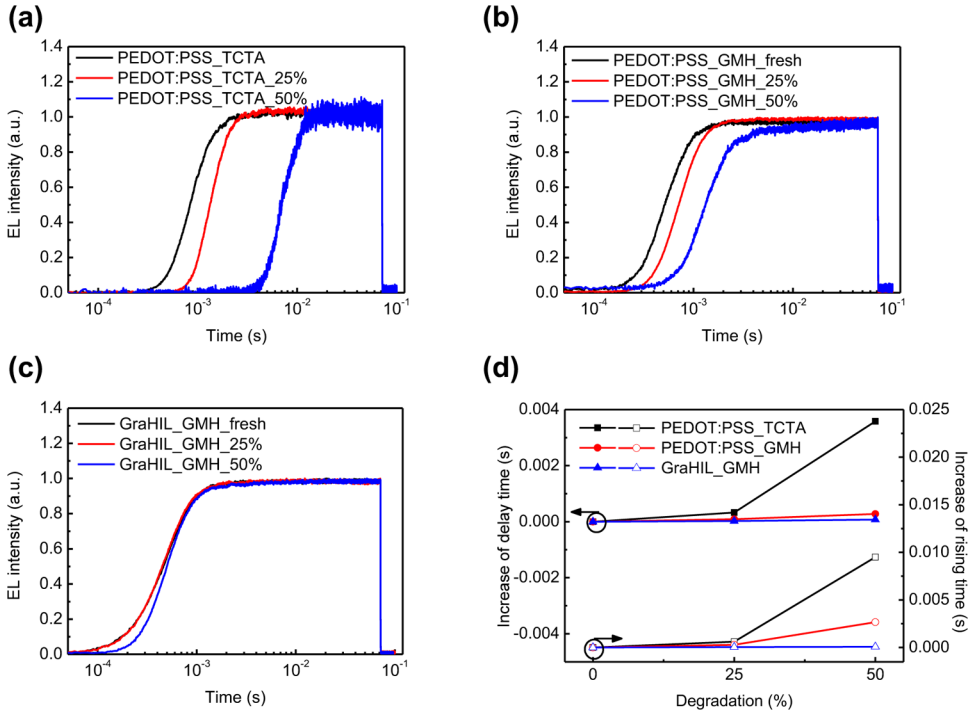

Figure 6. Transient EL rising characteristics of OLEDs that use (a) the TCTA single-host with PEDOT:PSS and TCTA:TPBI gradient mixed-host EML with (b) PEDOT:PSS and (c) GraHIL at various degraded stages and (d) increase of delay time (closed symbols) and rising time (open symbols) defined as reaching time to 90% of saturated EL intensity of devices under device degradation (fresh, 25%, and 50% degraded stages of initial luminance under constant current operation).

peak capacitance gradually increased (5 to 5.7 V) despite similar V_{peak} values. Even though the device degradation of the OLED that uses the GMH-EML with GraHIL also slightly retarded and decreased the peak capacitance, V_c did not change significantly (Figure 5c,d); this result means that charge carrier balance in the OLED that uses the TCTA:TPBI GMH-EML with GraHIL was not significantly changed even under device degradation compared with those of the others.

DOI: 10.1021/acsami.5b11791
ACS Appl. Mater. Interfaces 2016, 8, 6152−6163

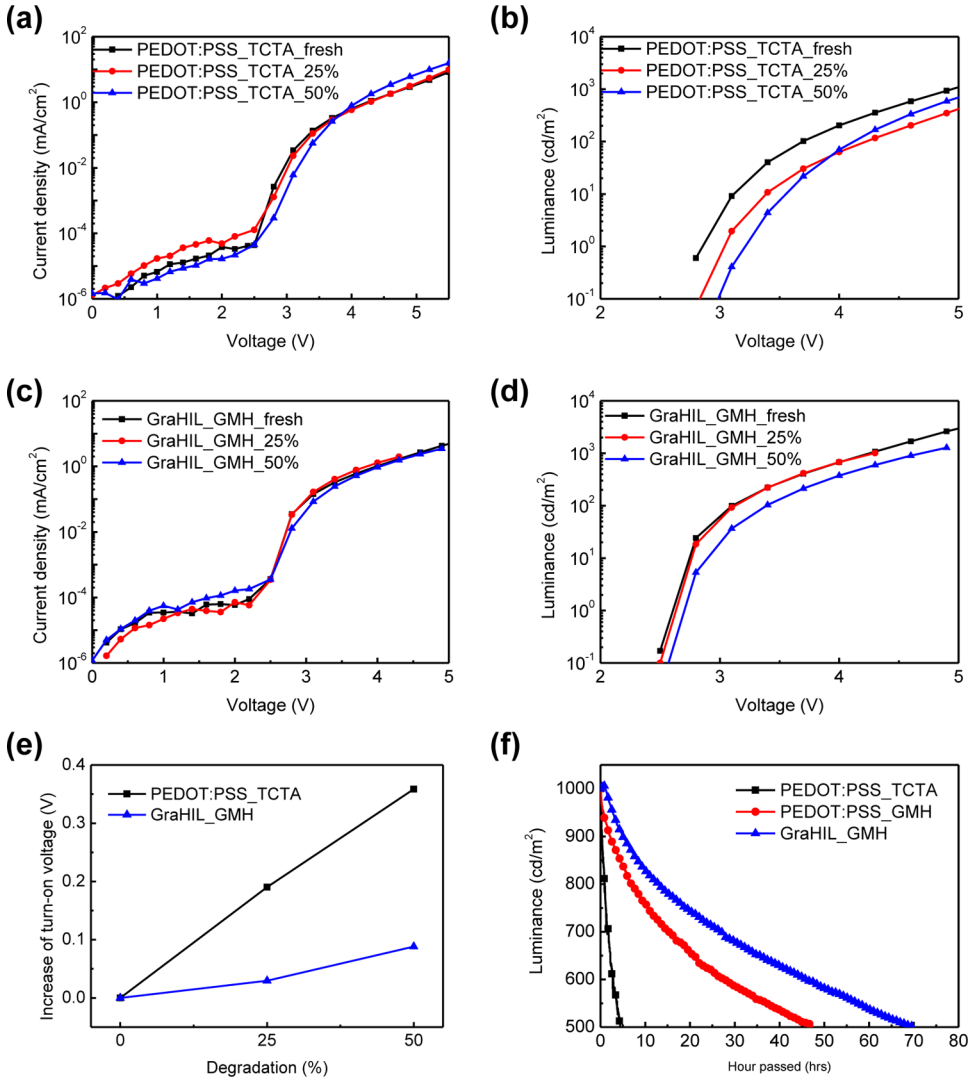

Figure 7. (a) Current density and (b) luminance versus voltage characteristics of OLEDs that use a TCTA single-host EML with PEDOT:PSS; (c) current density and (d) luminance versus voltage characteristics of OLEDs that use the TCTA:TPBI gradient mixed-host EML with GraHIL; (e) increase of turn-on voltage (i.e., voltage required to emit ∼1 cd m^{-2}) of OLEDs that use TCTA single-host EML with PEDOT:PSS and TCTA:TPBI gradient mixed-host EML with GraHIL at various degraded stages (fresh, 25%, and 50% degradation of luminance from the initial value under constant-current operation); (f) operational lifetimes of simple-structured OLEDs that use different materials under constant current operation.

Transient EL characterization also revealed changes related to the charge injection and transport under device degradation according to host systems of EML and HILs (Figure 6). OLED that uses the TCTA single-host EML with PEDOT:PSS gradually and significantly delayed EL rising under device degradation: t_d increased by $\sim 3.8 \times 10^{-3}$ s, and t_s increased by 9.5×10^{-3} s (Figure 6a,d). Device degradation under constant current made the device that uses the GMH-EML with PEDOT:PSS still exhibit delayed t_d and t_s compared to those of the nondegraded device, but the amount of both t_d and t_s increases (2.8×10^{-4} and 2.7×10^{-3} s) are smaller than those in the device with the TCTA single-host EML in transient EL (Figure 6b,d). In contrast, it is noticeable that the change of transient EL rising characteristics was negligible in the device that uses GMH-EML with GraHIL (increase of t_d: $\sim 7.5 \times 10^{-5}$ s; increase of t_s: $\sim 7 \times 10^{-5}$ s; Figure 6c,d). Because the change of transient EL characteristics represents the variations of electroluminescent properties in OLEDs related to the charge carrier injection and transport, large increases of t_d and t_s reflect severe degradation of charge injection to make charge carriers meet in the EML and charge transport to keep charge balance between electrons and holes. These results according to devices using different host systems and HILs concur with those of *C*–*V* characterization. The inefficient hole injection of the device with PEDOT:PSS increasingly degraded charge carrier injection and transport during continuous device operation. Furthermore, the use of TCTA unipolar single-host EML accelerates device degradation related to charge injection and transport with PEDOT:PSS because of severe charge imbalance and formation of a narrow recombination zone close to the interface between EML and ETL. The use of bipolar GMH-EML greatly facilitates charge injection and transport into the EML, thereby forming a broad recombination zone far from the interface. Concurrently, the reduction of hole injection energy barrier between HIL and EML by using GraHIL also significantly prevents degradation of the charge injecting and transporting capability of OLEDs compared to those that use PEDOT:PSS.

DOI: 10.1021/acsami.5b11791
ACS Appl. Mater. Interfaces 2016, 8, 6152–6163

$I-V-L$ tests revealed decreased electroluminescent properties of OLEDs; this decrease represents degradation in the capability to inject and transport charge carriers into the EML (Figure 7). At low voltages, current density and luminance characteristics decreased gradually in the OLED that uses the GMH-EML with GraHIL but decreased more severely in the OLED that uses the TCTA single-host EML with PEDOT:PSS (Figure 7a–d). The V_{to}s were obviously different between the two devices (Figure 7e). In OLED that uses the TCTA single-host EML with PEDOT:PSS, V_{to} increased significantly by ∼0.36 V, but in OLEDs that use GMH-EML and GraHIL, V_{to} increased by only ∼0.09 V; the difference indicates that charge injection and transport at low voltage under device operation degraded more in the former device than in the latter. The noticeably degraded electroluminescent properties of the former device at low voltages can be attributed to significant trap formation at the charge carrier injection interfaces;[27] after the trap states are filled at low voltages, the current density and luminance can be recovered at high voltages. The large difference in luminance characteristics can be attributed to the influences of exciton quenching including TTA and TPA due to the narrow recombination zone becoming crowded by charge carriers and excitons. Therefore, the fast decrease of luminance under constant current operation is caused by charge imbalance due to inefficient charge injection and a narrow recombination zone close to the interface of the OLED that uses the TCTA with PEDOT:PSS (Figure 7f). The surface enriched insulating PFI layer of GraHIL can effectively block the exciton quenching caused by PEDOT:PSS at the HIL/EML interface, and this capability of GraHIL was demonstrated in our previous simplified OLEDs.[16] When excitons generated in the EML diffuse or migrate to close proximity of the PEDOT:PSS layer (strong exciton quencher), exciton dissociation induced by (bi)polarons in doped PEDOT or nonradiative energy transfer from excitons generated in the EML to the doped PEDOT can reduce EL efficiencies of OLEDs.[16] The exciton quenching by the PEDOT:PSS can strongly influence the EL properties in the simple-structured OLEDs because EML is positioned directly on top of the HIL. However, in this work, both the TCTA single-host EML and the GMH-EML do not form a recombination zone near the HIL/EML interface because of unipolar hole transporting properties of TCTA and a shallower LUMO energy level (∼2.3 eV) of TCTA than that of TPBI (∼2.7 eV). Therefore, the contribution of GraHIL to blocking surface exciton quenching near the HIL/EML interface can be downsized in this degradation analysis work. On the other hand, other exciton quenching mechanisms related to the charge or exciton population including TTA and TPA can be considered as main factors in this work because the TCTA unipolar single-host EML have inefficient charge injection, cause charge imbalance, and form a narrow recombination zone at the EML/ETL interface in the simple-structured OLEDs. Therefore, the difference of EL properties between the TCTA single-host device and the GMH-EML device during operation can be attributed to the enhanced charge injection, better charge balance, and broad recombination zone in the EML.

The OLED that uses the GMH with PEDOT:PSS had longer lifetimes than that with the TCTA single-host EML. The half-lifetime (LT_{50}) under constant current which initially emits luminance ∼1000 cd m^{-2} was more than 10 times longer (∼47.8 h) in the OLED that uses the GMH with PEDOT:PSS than in OLEDs that use the TCTA single-host EML (∼4.4 h) (Figure 7f, Table 1). Furthermore, the use of GraHIL in the OLED that uses the GMH-EML further increased this LT_{50} to ∼70.7 h because GraHIL provides efficient charge injection into the TCTA for balanced charge transport, which forms a broad recombination zone. In addition, the surface-enrichment in PFI layer blocks metal atoms including In and Sn released from the ITO anode, which is easily etched by the acidic PEDOT:PSS polymer dispersion.[12,20]

Degradation Mechanism. Due to low carrier concentration of organic materials, charge carrier injection into organic layers throughout the injection contact is one of the most important factors that determine carrier profiles and dynamics in OLEDs. Therefore, the electrical and luminescent properties of OLEDs can be significantly changed by controlling the injection contact. Because the hole injection energy barrier is large, the PEDOT:PSS HIL can not inject sufficient holes into the EML, so in simple-structured OLEDs, holes are not injected and accumulate at the HIL/EML interface; electrons in the unipolar TCTA single-host EML accumulate at the EML/ETL interface because TCTA has a shallower LUMO energy level (∼2.3 eV) than does TPBI (∼2.7 eV) and very low electron mobility.[21,27] Accumulation of uninjected charge carriers at one injecting interface can cause additional accumulation of counter-charge carriers which would otherwise have recombined with injected charges in the EMLs. These space charges caused by charge accumulation in organic materials cause charged excitations such as polarons or bipolarons in the organic materials.[29,30] Charged excitations like bipolarons generated in organic materials can act as charge-trapping sites and nonradiative recombination centers.[12,27,31,32] The trap formation degrades effective charge carrier mobility and transport in organic materials and thereby increases operating voltage in OLEDs. Furthermore, formation of interfacial traps alters the electric field distribution in the devices, so change in the injection properties at the interfaces can increase under device operation. Accumulation of charged species also leads to exciton quenching such as polaron-exciton quenching and a consequent decrease in the luminance and LEs of OLED.[33,34]

The distribution of excitons and charge carriers may be another important factor that affects intrinsic degradation of OLEDs. The narrow recombination zone that forms very close to the heterointerface in the unipolar single-host EML also reduces the luminescent characteristics and LEs of OLEDs by influencing additional exciton quenching such as TTA and TPA (Figure 8a). The accumulated charged species and narrow recombination zone caused by the inefficient charge injection into the EML and imbalanced (or unipolar) transport of EML in simple-structured OLEDs increasingly degrades the charge injection and transport capability and luminescence of OLEDs as devices are operated, that is demonstrated by $C-V$, transient EL, and $I-V-L$ characterizations of devices that use PEDOT:PSS and the TCTA single-host EML. As a result, operation at constant current rapidly increases the voltage and decreases the luminance and, consequently, reduces their lifetimes. In contrast, the GraHIL provides efficient hole injection into the EML without HTL in simple-structured OLEDs and effectively blocks the metal atoms that diffuse from the ITO anode into organic layers; metal impurities in the organic layer can also form charge-trapping sites and nonradiative recombination centers during device operation.[6,35,36] The GMH-EML also greatly facilitates both hole and electron injection/transport to the recombination zone because the ratio

DOI: 10.1021/acsami.5b11791
ACS Appl. Mater. Interfaces 2016, 8, 6152–6163

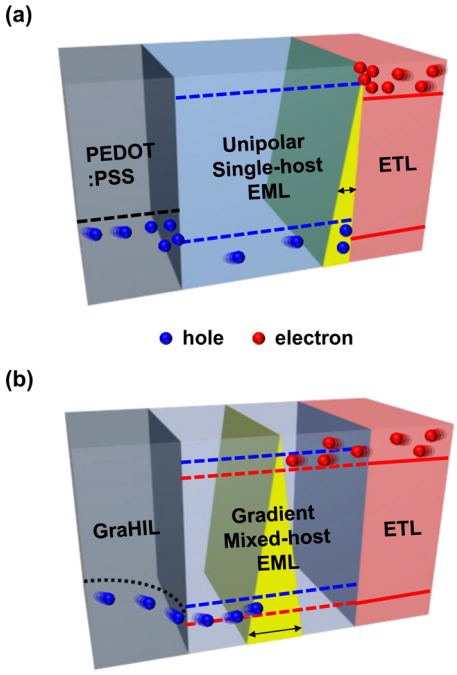

Figure 8. Schematic illustrations of operational degradation mechanism related to EML using (a) the TCTA single-host and (b) the TCTA:TPBI gradient mixed-host system.

of the hole-transporting host material to the electron-transporting host material changes gradually throughout the EML. In addition, OLEDs that use the GMH-EML distribute excitons and charge carriers to a broad recombination zone and shift the recombination zone from near the interface toward the center of the EML thereby effectively decreasing nonradiative recombinations related to density of charges and excitons (Figure 8b). Therefore, the combined use of GraHIL and the GMH-EML can significantly improve electrical and luminescent properties and operational stability of OLEDs compared to those of OLEDs with PEDOT:PSS and the TCTA single-host EML.

CONCLUSIONS

We used nondestructive analyses ($C-V$, transient EL, $I-V-L$, and lifetime measurement) to investigate the influences of the injection contact and the host system of EML on EL properties and operational stability of simple-structured phosphorescent OLEDs that use various host materials and compositions by varying the hole injection materials (GraHIL or PEDOT:PSS). To realize simple-structured OLEDs that are both highly efficient and stable, the major factors that influence EL properties and stability of OLEDs that should be considered are (1) efficient charge carrier injection through injection contact and (2) a broad recombination zone formed far from the hetero-organic interfaces of the EML. The improved surface WF (~5.95 eV) of GraHIL facilitates hole injection into host materials in the EML without HTL and, thereby, reduces operating voltage and increases EL efficiency compared to PEDOT:PSS. Using the GMH-EML also lets both charge carriers be easily injected and transported to the recombination zone in the EML; formation of a broad recombination zone at center of the EML is another major advantage of the GMH-EML compared to devices that have a unipolar single-host EML. An inefficient charge carrier injection and narrow recombination zone near the interface in OLEDs that use the unipolar single-host EML with PEDOT:PSS accelerated deterioration of charge carrier injection and transport and EL properties during device operation; the mechanism involves severe accumulation of charge trapping and exciton quenching space charges in organic layers. We concluded that a combined use of the GMH-EML system and high-performance HIL (or GraHIL) was very effective to achieve higher efficiency and longer device lifetime in simplified OLEDs. Our approaches to verify the major factors that determine electrical and luminance characteristics of simple-structured OLEDs can guide development of efficient, stable, and inexpensive OLEDs.

ASSOCIATED CONTENT

Supporting Information

The Supporting Information is available free of charge on the ACS Publications website at DOI: 10.1021/acsami.5b11791.

Deposition steps for gradient mixed-host EML, device characteristics of simple-structured OLEDs that use CBP single-host emitting layer, electroluminescence spectra of OLEDs using various kinds of host systems, and normalized capacitances versus voltage characteristics of simple-structured OLEDs that use various kinds of host systems in EML. (PDF)

AUTHOR INFORMATION

Corresponding Author

*Tel: 82-54-279-2151. Fax: 82-54-279-2399. E-mail: twlee@postech.ac.kr or taewlees@gmail.com.

Author Contributions

T.-H.H. designed and conducted all experiments and characterizations, analyzed all of the experimental results, and prepared the manuscript. Y.-H.K. assisted with the experiments. M.H.K. and W.S. discussed the experimental results. T.-W.L. initiated the study, designed all the experiments, analyzed all the data, and prepared the manuscript. All authors in this paper discussed the experiments and the results of the paper.

Notes

The authors declare no competing financial interest.

ACKNOWLEDGMENTS

This work was supported by the display research center program of Samsung Display Co., Ltd., and a National Research Foundation of Korea (NRF) grant funded by the Korean government (MSIP) (NRF-2013R1A2A2A01068753).

REFERENCES

(1) Kido, J.; Kimura, M.; Nagai, K. Multilayer White Light-Emitting Organic Electroluminescent Device. *Science* **1995**, *267*, 1332−1334.
(2) Shen, Z.; Burrows, P. E.; Bulovic, V.; Forrest, S. R.; Thompson, M. E. Three-color, Tunable, Organic Light-Emitting Devices. *Science* **1997**, *276*, 2009−2011.
(3) Baldo, M. A.; O' Brien, D. F.; You, Y.; Shoustikov, A.; Sibley, S.; Thomson, M. E.; Forrest, S. R. Highly Efficient Phosphorescent Emission from Organic Electroluminescent Devices. *Nature* **1998**, *395*, 151−154.
(4) Friend, R. H.; Gymer, R. W.; Holmes, A. B.; Burroughes, J. H.; Marks, R. N.; Taliani, C.; Bradley, D. D. C.; Dos Santos, D. A.; Brédas, J. L.; Lögdlund, M.; Salaneck, W. R. Electroluminescence in Conjugated Polymers. *Nature* **1999**, *397*, 121−128.
(5) Reineke, S.; Lindner, F.; Schwartz, G.; Seidler, N.; Walzer, K.; Lussem, B.; Leo, K. White Organic Light-Emitting Diodes with Fluorescent Tube Efficiency. *Nature* **2009**, *459*, 234−238.

DOI: 10.1021/acsami.5b11791
ACS Appl. Mater. Interfaces 2016, 8, 6152−6163

(6) Han, T.-H.; Lee, Y.; Choi, M.-R.; Woo, S.-H.; Bae, S.-H.; Hong, B. H.; Ahn, J.-H.; Lee, T.-W. Extremely Efficient Flexible Organic Light-Emitting Diodes with Modified Graphene Anode. *Nat. Photonics* **2012**, *6*, 105−110.
(7) Uoyama, H.; Goushi, K.; Shizu, K.; Nomura, H.; Adachi, C. Highly Efficient Organic Light-Emitting Diodes from Delayed Fluorescence. *Nature* **2012**, *492*, 234−238.
(8) So, F.; Kondakov, D. Degradation Mechanisms in Small-Molecule and Polymer Organic Light-Emitting Diodes. *Adv. Mater.* **2010**, *22*, 3762−3777.
(9) Aziz, H.; Popovic, Z. D.; Hu, N.-X.; Hor, A.-M.; Xu, G. Degradation Mechanism of Small Molecule-Based Organic Light-Emitting Devices. *Science* **1999**, *283*, 1900−1902.
(10) Aziz, H.; Popovic, Z. D. Degradation Phenomena in Small-Molecule Organic Light-Emitting Devices. *Chem. Mater.* **2004**, *16*, 4522−4532.
(11) Schaer, M.; Nüesch, F.; Berner, D.; Leo, W.; Zuppiroli, L. Water Vapor and Oxygen Degradation Mechanisms in Organic Light Emitting Diodes. *Adv. Funct. Mater.* **2001**, *11*, 116−121.
(12) Han, T.-H.; Song, W.; Lee, T.-W. Elucidating the Crucial Role of Hole Injection Layer in Degradation of Organic Light-Emitting Diodes. *ACS Appl. Mater. Interfaces* **2015**, *7*, 3117−3125.
(13) Sun, Y.; Giebink, N. C.; Kanno, H.; Ma, B.; Thompson, M. E.; Forrest, S. R. Management of Singlet and Triplet Excitons for Efficient White Organic Light-Emitting Devices. *Nature* **2006**, *440*, 908−912.
(14) Zhou, X.; Blochwitz, J.; Pfeiffer, M.; Nollau, A.; Fritz, T.; Leo, K. Enhanced Hole Injection into Amorphous Hole-Transport Layers of Organic Light-Emitting Diodes Using Controlled p-Type Doping. *Adv. Funct. Mater.* **2001**, *11*, 310−314.
(15) Kido, J.; Matsumoto, T. Bright Organic Electroluminescent Devices Having a Metal-Doped Electron-Injecting Layer. *Appl. Phys. Lett.* **1998**, *73*, 2866.
(16) Han, T.-H.; Choi, M.-R.; Woo, S.-H.; Min, S.-Y.; Lee, C.-L.; Lee, T.-W. Molecularly Controlled Interfacial Layer Strategy Toward Highly Efficient Simple-Structured Organic Light-Emitting Diodes. *Adv. Mater.* **2012**, *24*, 1487−1493.
(17) Murawski, C.; Leo, K.; Gather, M. C. Efficiency Roll-Off in Organic Light-Emitting Diodes. *Adv. Mater.* **2013**, *25*, 6801−6827.
(18) Lee, S. J.; Koo, J. R.; Lee, H. W.; Lee, S. E.; Yang, H. J.; Yoon, S. S.; Park, J.; Kim, Y. K. Effect of a Broad Recombination Zone with a Triple-Emitting Layer on the Efficiency of Blue Phosphorescent Organic Light-Emitting Diodes. *Electron. Mater. Lett.* **2014**, *10*, 1127−1131.
(19) Wang, Q.; Oswald, I. W. H.; Perez, M. R.; Jia, H.; Gnade, B. E.; Omary, M. A. Exciton and Polaron Quenching in Doping-Free Phosphorescent Organic Light-Emitting Diodes from a Pt(II)-Based Fast Phosphor. *Adv. Funct. Mater.* **2013**, *23*, 5420−5428.
(20) Lee, T.-W.; Chung, Y.; Kwon, O.; Park, J.-J. Self-Organized Gradient Hole Injection to Improve the Performance of Polymer Electroluminescent Devices. *Adv. Funct. Mater.* **2007**, *17*, 390−396.
(21) Sun, Y.; Forrest, S. R. High-Efficiency White Organic Light Emitting Devices with Three Separate Phosphorescent Emission Layers. *Appl. Phys. Lett.* **2007**, *91*, 263503.
(22) Shrotriya, V.; Yang, Y. Capacitance-Voltage Characterization of Polymer Light-Emitting Diodes. *J. Appl. Phys.* **2005**, *97*, 054504.
(23) Kang, J.-W.; Lee, S.-H.; Park, H.-D.; Jeong, W.-I.; Yoo, K.-M.; Park, Y.-S.; Kim, J.-J. Low Roll-Off of Efficiency at High Current Density in Phosphorescent Organic Light Emitting Diodes. *Appl. Phys. Lett.* **2007**, *90*, 223508.
(24) Barth, S.; Müller, P.; Riel, H.; Seidler, P. F.; Rieß, W.; Vestweber, H.; Bässler, H. Electron Mobility in Tris(8-hydroxyquinoline)aluminum Thin Films Determined via Transient Electroluminescence from Single- and Multilayer Organic Light-Emitting Diodes. *J. Appl. Phys.* **2001**, *89*, 3711.
(25) Nikitenko, V. R.; Arkhipov, V. I.; Tak, Y.-H.; Pommerehne, J.; Bässler, H.; Hörhold, H.-H. The Overshoot Effect in Transient Electroluminescence from Organic Bilayer Light Emitting Diodes: Experiment and Theory. *J. Appl. Phys.* **1997**, *81*, 7514.
(26) Helander, M. G.; Wang, Z. B.; Qiu, J.; Greiner, M. T.; Puzzo, D. P.; Liu, Z. W.; Lu, Z. H. Chlorinated Indium Tin Oxide Electrodes with High Work Function for Organic Device Compatibility. *Science* **2011**, *332*, 944−947.
(27) Kondakov, D. Y.; Sandifer, J. R.; Tang, C. W.; Young, R. H. Nonradiative Recombination Centers and Electrical Aging of Organic Light-Emitting Diodes: Direct Connection Between Accumulation of Trapped Charge and Luminance Loss. *J. Appl. Phys.* **2003**, *93*, 1108.
(28) Kahen, K. B. Rigorous Optical Modeling of Multilayer Organic Light-Emitting Diode Devices. *Appl. Phys. Lett.* **2001**, *78*, 1649.
(29) Dyreklev, P.; Inganas, O.; Paloheimo, J.; Stubb, H. Photoluminescence Quenching in a Polymer Thin-Film Field-Effect Luministor. *J. Appl. Phys.* **1992**, *71*, 2816−2820.
(30) Baldo, M. A.; Forrest, S. R. Interface-Limited Injection in Amorphous Organic Semiconductors. *Phys. Rev. B: Condens. Matter Mater. Phys.* **2001**, *64*, 085201.
(31) Popovic, Z. D.; Aziz, H. Reliability and Degradation of Small Molecule-based Organic Light-Emitting Devices (OLEDs). *IEEE J. Sel. Top. Quantum Electron.* **2002**, *8*, 362−371.
(32) Gärtner, C.; Karnutsch, C.; Lemmer, U.; Pflumm, C. The Influence of Annihilation Processes on the Threshold Current Density of Organic Laser Diodes. *J. Appl. Phys.* **2007**, *101*, 023107.
(33) Bolinger, J. C.; Traub, M. C.; Adachi, T.; Barbara, P. F. Ultralong-Range Polaron-Induced Quenching of Excitons in Isolated Conjugated Polymers. *Science* **2011**, *331*, 565−567.
(34) Wang, Q.; Aziz, H. Degradation of Organic/Organic Interfaces in Organic Light-Emitting Devices due to Polaron−Exciton Interactions. *ACS Appl. Mater. Interfaces* **2013**, *5*, 8733−8739.
(35) de Jong, M. P.; van IJzendoorn, L. J.; de Voigt, M. J. A. Stability of the Interface Between Indium-Tin-Oxide and Poly (3, 4-ethylenedioxythiophene)/Poly (styrenesulfonate) in Polymer Light-Emitting Diodes. *Appl. Phys. Lett.* **2000**, *77*, 2255.
(36) Sharma, A.; Andersson, G.; Lewis, D. A. Role of Humidity on Indium and Tin Migration in Organic Photovoltaic Devices. *Phys. Chem. Chem. Phys.* **2011**, *13*, 4381−4387.

DOI: 10.1021/acsami.5b11791
ACS Appl. Mater. Interfaces 2016, 8, 6152−6163